Metamaterial absorber-based sensor embedded into X-band waveguide

C. Sabah, O. Turkmen-Kucuksari and G. Turhan-Sayan

A novel metamaterial sensor, integrated with an X-band waveguide, is proposed for high-resolution measurements of variations in the dielectric constant and/or the thickness of a superstrate layer that covers a pair of absorber unit cells. Variations in superstrate parameters are potentially caused by physical, chemical or biological factors, and can be detected by measuring the corresponding shifts in the resonance frequency of the metamaterial sensor. It is estimated by simulation results that resolution levels as good as 1.1 μm change in thickness or 0.023 absolute change in relative permittivity of the sensing layer are feasible for a 10 MHz measurable shift in resonance frequency. Simulation results obtained for the fabricated prototype are verified experimentally with good agreement.

Introduction: Metamaterials (MTMs) are engineered structures possessing extraordinary features such as backward propagation, negative permittivity and/or negative permeability, which are not readily available in nature. For the past decade, MTMs have been extensively used for various applications [1] including absorbers [2–4], resonators [5], antennas [6] and sensors [7–9] with reduced electrical size and improved functionality. MTM absorber arrays are designed to minimise both reflected and transmitted power to yield maximum absorption at the resonance frequency. The majority of the MTM absorbers reported in the literature are designed for radome applications for which the fundamental challenge is to maintain sufficiently high absorption levels under arbitrary excitation conditions regarding the incidence direction and polarisation. Within a single-mode waveguide, on the other hand, the directions of *E*-field vector and the propagation vector are already known. Therefore, there is no need for complicated absorber topologies when the structure is embedded into a waveguide.

This Letter reports a proof of concept study for a novel MTM sensor which integrates a pair of simple absorber unit cells with an X-band waveguide to provide high-resolution sensing in physical, chemical and biological sensor applications. To the best of our knowledge, this investigation is the first one in the literature which combines the MTM absorber and MTM sensor phenomena in a simple and efficient manner. In the proposed sensor topology, the absorber unit cells are covered by a sensing superstrate of thickness (t_{sen}) and relative permittivity (ϵ_r), and placed within an X-band waveguide, which supports only TE_{10} mode over the single-mode bandwidth (which is from 6.56 to 13.73 GHz for the X-band waveguide used in this Letter). Variations in superstrate parameters lead to shifts in the resonance frequency of the sensor. Therefore, frequency shifts measured from the reflectance pattern can be used to estimate the thickness or relative permittivity of the superstrate.

The aim of the proposed sensor design is twofold. First, the superstrate may be composed of an unknown sample to be characterised through sensor measurements. Secondly, an initially known superstrate layer may be used to sense various external factors such as temperature, humidity or the presence of an external material (that can bind to the superstrate layer, for example), which can effectively modify the thickness and/or refractive index of the superstrate in some way.

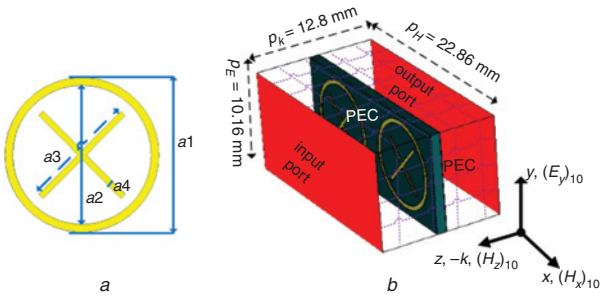


Fig. 1 *MTM absorber topology and simulation setup*

a Unit cell topology with dimensions for CW and CR resonators
b CST simulation setup within X-band waveguide

Design: The MTM absorber topology used in this sensor design is a simplified version of the absorber proposed in [4]. The basic unit cell geometry is composed of a cross-wire (CW) resonator and a circular-ring (CR) resonator printed on the front side of the FR4 substrate as shown in Fig. 1*a* with dimensions $a1 = 9$ mm, $a2 = 8.1$ mm, $a3 = 6.8$ mm and $a4 = 0.35$ mm. A pair of these unit cells is printed on the substrate, which is metal-plated on its back side to stop transmission. Copper metallisation on both sides of the substrate has a conductivity of 5.8×10^7 S/m and thickness of 0.035 mm, whereas the thickness, loss tangent and relative permittivity of the FR4 substrate are 1, 0.025 and 4.3 mm, respectively. The substrate perfectly fits within the X-band waveguide of dimensions 10.16, 12.8 and 22.86 mm in the *y*-, *z*- and *x*- directions, respectively, as shown schematically in Fig. 1*b*.

Simulation setup: Complex-valued scattering parameters (S_{11}, S_{21} etc.) of the MTM sensor are simulated using the commercial full-wave electromagnetic solver CST Microwave Studio, within a computational volume defined by the X-band waveguide dimensions. As indicated in Fig. 1*b*, perfect electric conductor boundary conditions are imposed at the boundary surfaces coinciding with the metal walls of the waveguide, whereas input and output ports are defined at those surfaces which are perpendicular to the propagation vector, $\boldsymbol{k}$.

Fabrication and experimental setup: The absorber structure is composed of twin unit cells, which was fabricated (see Fig. 2*a*) using the LPKF-ProtoMat-H100 circuit board plotter and placed within the X-band waveguide as shown in Fig. 3*a*. Then, measurements were conducted using the Agilent 8720D network analyser as shown in Fig. 3*b* to obtain the *S*-parameters of the structure.



Fig. 2 *Absorber unit cells and surface current density at resonance*

a Photograph of fabricated absorber unit cells
b Simulated surface current density at resonance frequency 11.9 GHz



Fig. 3 *Experimental setup*

a Placement of fabricated absorber unit into X-band waveguide
b *S*-parameter measurements using Agilent 8720D network analyser

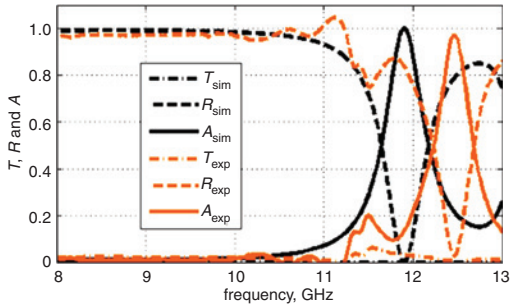


Fig. 4 *Simulation and experimental results for reflectance (R), transmittance (T) and absorption (A) of absorber-based MTM sensor embedded into X-band waveguide (for $t_{sen} = 0$ case)*

Results: Simulation results for reflectance $R(\omega) = |S_{11}|^2$, transmittance $T(\omega) = |S_{21}|^2$ and absorption $A(\omega) = 1 - R(\omega) - T(\omega)$ are plotted in Fig. 4 for the basic structure with zero thickness (i.e. for the $t_{sen} = 0$ case) for the sensing superstrate. Owing to the copper coating layer placed at the back side of the substrate, $T(\omega)$ turns out to be zero. Therefore,

as $R(\omega)$ is minimised, $A(\omega)$ reaches its maximum value of 0.999 (a case of an almost perfect absorber) at 11.9 GHz. As shown in Fig. 2*b*, the surface current density simulated over the CW resonator is strong. This indicates that the CW component of the absorber is primarily responsible for this electrically excited resonance at 11.9 GHz. The CR resonator, on the other hand, carries very small surface currents at this frequency, but it is still useful to provide fine tuning to minimise the return loss, $|S_{11}|$ of the structure.

Experimental results for reflectance, transmittance and absorption are also plotted in Fig. 4 showing good agreement with the simulation results. The measured resonance frequency is detected at 12.46 GHz (with an acceptable error of 4.7%) and the absorption peak is measured as 0.971 (with a small error of 2.8%).

Sensor resolution: For the purpose of sensor resolution assessment, two different sets of simulations were designed. First, the thickness (t_{sen}) of the sensing superstrate was kept constant at 0.1 mm. The $|S_{11}|$ spectra were simulated for different values of superstrate permittivity, $\varepsilon_r = 1$, 2,…, 6. The results are plotted in Fig. 5 where the case $\varepsilon_r = 1$ implies the absence of superstrate with $f_0 = 11.9$ GHz as previously shown in Fig. 4. The resonance frequency is shifted to lower values as the permittivity of the superstrate is increased. Variation of the resonance frequency with respect to sensing layer permittivity is plotted in the inset of Fig. 5 revealing the fact that sensor resolution gets better as ε_r decreases. For a measurable shift of $\Delta f_0 = 10$ MHz in resonance frequency, the smallest measurable variation in relative permittivity ($\Delta\varepsilon_r$) assumes its best value of 0.023 in the range $1 < \varepsilon_r < 2$. This is the sensor's best resolution regarding the variations in the superstrate permittivity. This value increases to 0.05 in the range $2 < \varepsilon_r < 5$ and it becomes 0.077 in the range $5 < \varepsilon_r < 6$ for $\Delta f_0 = 10$ MHz resonance shift.

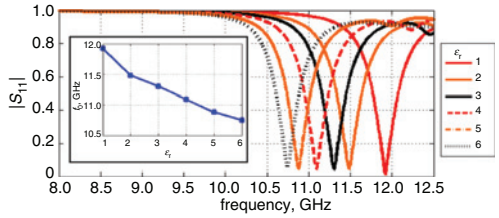


Fig. 5 *Insertion loss spectra of MTM sensor for different values of superstrate permittivity*

Inset: Variation of resonance frequency with relative permittivity of sensing superstrate for $t_{sen} = 0.1$ mm

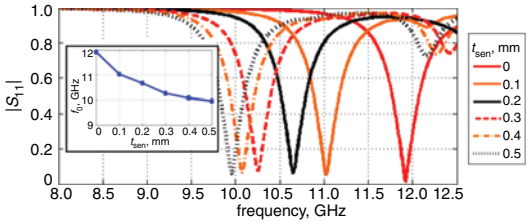


Fig. 6 *Insertion loss spectra of MTM sensor for different values of superstrate thickness*

Inset: Variation of resonance frequency with sensing superstrate thickness for $\varepsilon_r = 4.3$

Secondly, the relative permittivity (ε_r) of the superstrate was kept constant at 4.3. The $|S_{11}|$ spectra were simulated for different values of superstrate thickness (for $t_{sen} = 0$, 0.1, 0.2,…, 0.5 mm), and the results are plotted in Fig. 6 (obviously, no superstrate exists for the case $t_{sen} = 0$ for which $f_0 = 11.9$ GHz). The resonance frequency is shifted to lower values as the thickness of the superstrate is increased. Variation of the resonance frequency with respect to sensing layer thickness is plotted in the inset of Fig. 6 revealing the fact that sensor resolution improves as the sensing superstrate becomes thinner. For a measurable shift of $\Delta f_0 = 10$ MHz in resonance frequency, the smallest measurable variation in superstrate thickness (Δt_{sen}) assumes its best value of 1.1 μm in the range $t_{sen} < 0.1$ mm. This is the sensor's best resolution regarding the variations in the thickness of the sensing superstrate layer at the $\varepsilon_r = 4.3$ level. This value increases to 2.6, 5.5 and 9.1 μm for the ranges (0.1–0.3), (0.3–0.4) and (0.4–0.5) mm of parameter t_{sen}, respectively.

Conclusion: A novel absorber-based and waveguide-integrated MTM sensor design is demonstrated in this Letter for high-resolution sensing through the measurements of thickness and relative permittivity of a 'sensing' superstrate. The suggested MTM sensor is electrically small, geometrically simple, easy to fabricate, highly sensitive and has the potential of being useful for a wide range of sensing applications.

Acknowledgments: This work is partly supported by the METU-NCC under grant number BAP-FEN-13-D-4. Fabrication and measurement tasks were completed in the EEE Labs of METU-Ankara.

© The Institution of Engineering and Technology 2014
13 May 2014
doi: 10.1049/el.2014.1753
One or more of the Figures in this Letter are available in colour online.

C. Sabah (*Department of Electrical and Electronics Engineering, Middle East Technical University – Northern Cyprus Campus, Kalkanli, Guzelyurt, TRNC / Mersin 10, Turkey*)

O. Turkmen-Kucuksari and G. Turhan-Sayan (*Department of Electrical and Electronics Engineering, Middle East Technical University, Cankaya, Ankara 06800, Turkey*)

E-mail: oznurturkmen@gmail.com

O. Turkmen-Kucuksari: Also with the Department of Electronics and Telecommunications Engineering, Kocaeli University, Kocaeli, Turkey

References

1 Capolino, F.: 'Applications of metamaterials' (CRC Press, Boca Raton, FL, USA, 2009)
2 Bilotti, F., Nucci, L., and Vegni, L.: 'An SRR-based microwave absorber', *Microw. Opt. Technol. Lett.*, 2006, **48**, pp. 2171–2175
3 Landy, N.I., Sajuyigbe, S., Mock, J.J., Smith, D.R., and Padilla, W.J.: 'A perfect metamaterial absorber', *Phys. Rev. Lett.*, 2008, **100**, pp. 207402–207404
4 Dincer, F., Karaaslan, M., Unal, E., Delihacioglu, K., and Sabah, C.: 'Design of polarization and incident angle insensitive dual-band metamaterial absorber based on isotropic resonators', *Prog. Electromagn. Res.*, 2014, **144**, pp. 123–132
5 Turkmen, O., Ekmekci, E., and Turhan-Sayan, G.: 'Nested U-ring resonators: a novel multi-band metamaterial design in microwave region', *IET Microw. Antennas Propag.*, 2012, **6**, pp. 1102–1108
6 Turkmen, O., Turhan-Sayan, G., and Ziolkowski, R.W.: 'Single, dual and triple-band metamaterial-inspired electrically small planar magnetic dipole antennas', *Microw. Opt. Technol. Lett.*, 2014, **56**, pp. 83–87
7 Schüßler, M., Mandel, C., Puentes, M., and Jakoby, R.: 'Metamaterial inspired microwave sensors', *IEEE Microw. Mag.*, 2012, **13**, pp. 57–68
8 Sabah, C., and Roskos, H.G.: 'Broadside-coupled triangular split-ring-resonators for terahertz sensing', *Eur. Phys. J. Appl. Phys.*, 2013, **61**, (1–4), p. 103506
9 Ekmekci, E., and Turhan-Sayan, E.: 'Multi-functional metamaterial sensor based on a broad-side coupled SRR topology with a multilayer substrate', *Appl. Phys. A, Mater.*, 2013, **110**, pp. 189–197